Hindawi
Journal of Sensors
Volume 2021, Article ID 8871893, 10 pages
https://doi.org/10.1155/2021/8871893

Research Article

Development of Optic-Electric Hybrid Sensors for the Real-Time Intelligent Monitoring of Subway Tunnels

Fu-guang Zhu,[1] Dong-sheng Xu ,[2] Rui-shan Tan,[1] Bin Peng,[1] He Huang,[1] and Zhuo-wen Liu[2]

[1]*Hubei Electric Power Survey and Design Institute co., Ltd., Xinqiaosi Rd. Wuhan 430040, China*
[2]*School of Civil Engineering and Architecture, Wuhan University of Technology, 122 Luoshi Rd, Wuhan 430070, China*

Correspondence should be addressed to Dong-sheng Xu; dsxu@whut.edu.cn

Received 1 September 2020; Accepted 17 June 2021; Published 12 July 2021

Academic Editor: Pawel Malinowski

The settlement and deformation monitoring of subway tunnels had difficult in long-distance and real time measurement. This study proposed an optic-electric hybrid sensor based on infrared laser ranging technology and cable-sensing technology. The working principle, hardware layer, design details, laboratory calibration and field validation were presented and discussed. The optic-electric hybrid sensor implemented the real-time intelligent analysis modulus for the whole system which could analysis the measurement errors and improve the accuracy. The laboratory calibration tests were carried out and the results shown that the hybrid sensors had measurement resolution of 1 mm with the maximum measurement range of 100 m. A remote real-time intelligent monitoring system is established based on the hybrid sensors. The system contains an edge computing module, real-time communication module and warning light signal with three colors. The stability of data acquisition and transmission of the intelligent control monitoring system under long-term conditions was examined. Test results shown that the system was quite stable for the long-term measurement. The whole system was verified in a constructing subway tunnel of Wuhan Metro Line 8, China. According to the field monitoring results, the deformations and the state of health safety of the tunnel was evaluated. The results of this study could provide useful guidance for tunnel deformation monitoring and has great practical value in civil engineering.

1. Introduction

In recent years, the construction of infrastructures had been further accelerated, and a large number of tunnels had been built. Safety accidents caused huge economic property lose, which caused by tunnel settlement and deformation. Therefore, it was important that the monitoring of the tunnel during construction and operation. At present, the main domestic tunnel deformation monitoring instruments were electronic total station, laser convergence meter, traditional steel rule convergence meter [1–5]. The mentioned various monitoring instruments had high measurement accuracy, but due to their few measurement points, it was impossible to establish a three-dimensional space model of the tunnel, and it was difficult to intuitively and comprehensively reflect the actual deformation of the tunnel. All of the above monitoring instruments have good performance during the construction phase [6–10]. Then, tunnel deformation safety monitoring loopholes were caused. When the tunnel was put into operation, the traditional method no longer meets the actual situation. Therefore, it was necessary to establish a deformation monitoring system with more accurate, simpler, smarter, relatively cost-effective, and less interfere the normal operation of the tunnel [11].

Many researchers have been devoted lots of efforts to develop new approaches for the tunnel deformation monitoring, such as Xie et al. [12] developed a measurement method based on the establishment of a three-dimensional model of the tunnel to obtain the relative deformation information of the tunnel's full cross section using laser ranging

technology. Liu et al. [13] proposed a three-dimensional laser scanning technology in tunnel deformation monitoring, and studied the sensitivity of the experimental factors to tunnel deformation analysis, greatly reduce the error fluctuation range of the monitoring results; Dong et al. [14] proposed a method for monitoring the settlement and deformation of the overlying layer of the tunnel using distributed optical fiber, the feasibility of distributed optical fiber in monitoring the longitudinal settlement of overlying rock and soil during tunnel construction was verified; Hou et al. [15] proposed a tunnel settlement inversion model based on distributed optical fiber strain, linked the optical fiber strain curve to the tunnel settlement curve; Du et al. [16] studied the effect of tide level changes on the settlement and convergence deformation of the cross-river shield tunnel based on tunnel deformation monitoring data. Yang [17] proposed a distributed long-gauge fiber grating for real-time monitoring of tunnel settlement deformation. However, due to the complex geological conditions at the tunnel site, the existing monitoring methods still have technical limitations [18–23], such as some monitoring system has limitation of long-distance signal transmissions; while some monitoring methods were costly [24–30].

This study proposes a practical tunnel deformation monitoring approach with optic-electric hybrid sensing approach. Based on the laser ranging technology and cable sensing technology, a real-time monitoring and early warning system for tunnel deformation was developed. The system can transmit tunnel deformation data in real time, and intelligently identify the deformation with automatically feedback. The proposed system was installed in the field of tunnel deformation monitoring of Xiaohongshan station of Wuhan metro line.

2. Intelligent Monitoring and Early-Warning System

2.1. System Diagram. Figure 1 shows the overall functional framework of the intelligent monitoring and early warning system. As shown in the figure, the entire system consists of four parts: Data acquisition and transmission system (DATS), Data processing and control system (DPCS), Intelligent early warning system (IEWS) and inspection and maintenance system (IMS). The DPCS transmits the control signal to the DATS. The DATS starts to work according to the signal content. First, the data is collected by the sensor, the data is preprocessed, and finally the data is transmitted to the DPCS. The DPCS stores and transmits the measurement data to the intelligent early warning system. IEWS provides early warning of the danger level by analyzing the measurement data. The IMS is used for debugging and maintenance.

Each sensor node consisted of the long-distance wireless signal transmission function to form a cooperative working system. The control system implemented real-time intelligent analysis modulus for the whole system according to the program set by the developer. The wireless transmission system can realize remote real-time control of the system, which greatly reduces the difficulty of maintenance and management in the complex site environment of the tunnel.

2.2. Hardware Layer. Figure 2 presents the overall hardware framework of the intelligent monitoring and early warning system. The infrared laser sensor and electrical tunnel convergence measurement instrument were proposed with automatic data collection and wireless transmission modulus. Thus, the hardware can achieve functions of data collection, preprocessing and signals transmission. The intelligent control warning lamp integrated data processing and control system and the intelligent analysis for the warning system. An intelligent control warning light can control multiple infrared laser rangefinders and cable convergence instruments, which greatly simplifies the operation process and reduces the operating cost of the system.

2.2.1. Data Acquisition and Transmission System. Figure 3 shows the hardware composition of optic-electric hybrid sensing system with the infrared laser sensor and electrical convergence sensing element. The optic-electric hybrid sensing system mainly included infrared laser sensor, electrical convergence sensor, single-chip microcomputer, buck module, communication module and battery. The program was installed into the single-chip microcomputer which would used to control the measurement frequency and signal transmissions. The buck and power modulus were used for stable power supply and power warning of the sensing node. The infrared laser sensor has a range of 100 m and an accuracy of 1 mm. The electrical convergence sensor has a range of 1.2 m and an accuracy of 1 mm. Two rechargeable lithium batteries were installed in the sensing node. After the power was turned on, a wireless connection was established with the intelligent control warning light through a communication module. The intelligent control node would trigger a signal to control the working status of the infrared laser sensors. The infrared laser sensor can be set as the working mode and sleep mode (i.e. energy saving mode). All the data would be recorded in the sensing nodes.

2.2.2. Control and Intelligent Early Warning System. Figure 4 shows the intelligent control warning system which composed of single chip microcomputer, timing module, indicator module, power supply module, buck module, communication module and memory. The intelligent control warning system was used to remotely control the working status of the sensors installed on the surface of the tunnel. The data was received and recorded in the warning system. Based on the recorded data, the state of health (SoH) of the subway tunnel would be analyzed and determined. Then, the SoH status would be transmitted and converted to the warning lights which could be directly and easily observed by the in-site workers and site mangers. The warning signals were classified as three levels with three different colors, such as red, yellow and blue, which were used to indicate three different SoH states of very dangerous, dangerous and safe state, respectively.

The working principle of the whole system can be divide into four steps: firstly, after the power was turned on, the intelligent control warning light transmits signals to the optic-electric hybrid sensing chips to wake up the sensor. Then, all the sensors would be self-checked to make sure the working condition was prepared. Secondly, all the sensing nodes would

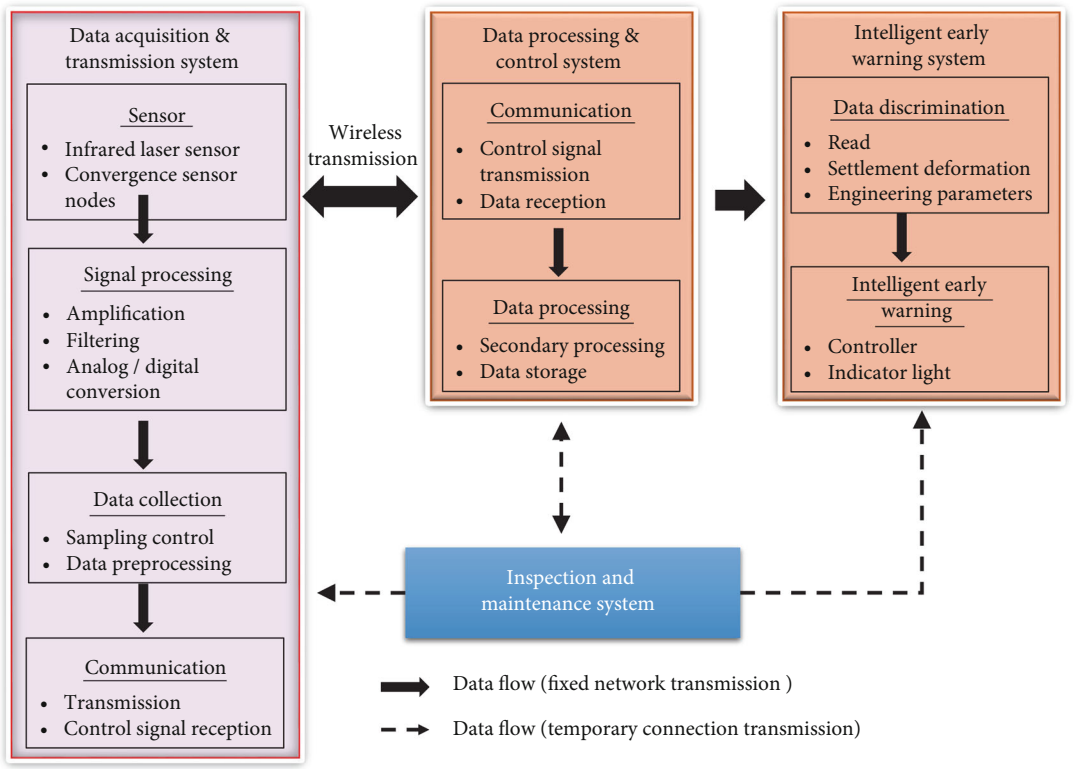

Figure 1: System diagram of the intelligent monitoring and early-warning system with optic-electric hybrid sensing.

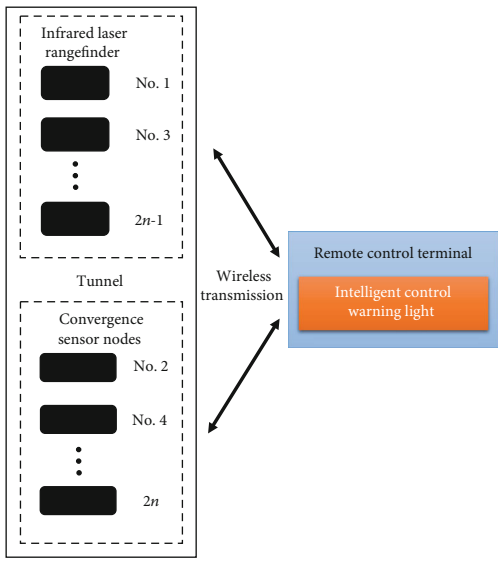

Figure 2: Diagram of the intelligent control warning system.

be conducted several measurements to minimize errors. After the measurement was completed, the laser rangefinder sensors would be turned into the sleep mode until the next measurement cycle. Thirdly, the measured results were transmitted and recorded in the memory storage. Finally, the data would be analyzed in the intelligent control modulus.

After each test instrument was installed, the intelligent control warning light controls each sensor in sequence according to the set procedure, transmits and stores the measurement data of each measurement point in real time, and lights up according to the rules to monitor the tunnel deformation and settlement in real time. In this study, the frequency of data acquisition would be adapted to the health status, such as in the higher dangerous status, the frequency of data acquisition was 1 minute per time. The data will be taken at the interval of 5 minutes in yellow warning status. In health state, the data for all sensors would be taken at the interval of 30 minutes. The frequency of data acquisition can be changed according to various projects.

3. Laboratory Test

This part conducts laboratory tests on the Intelligent monitoring and early-warning system, and studies the measurement error of the system under different monitoring distances, the fluctuation range of the error, and the stability of the system under long-term work.

3.1. Analysis of Systematical Errors. The optic-electric hybrid sensing for tunnel settlement was tested in the laboratory. In order to validate the accuracy at different measurement distances, the sensors were carefully examined with various distances. Figure 5 shows the calibration results of the sensors. Further detailed calibration tests were carried out at different distances of 5 m, 30 m and 50 m. The calibrations were

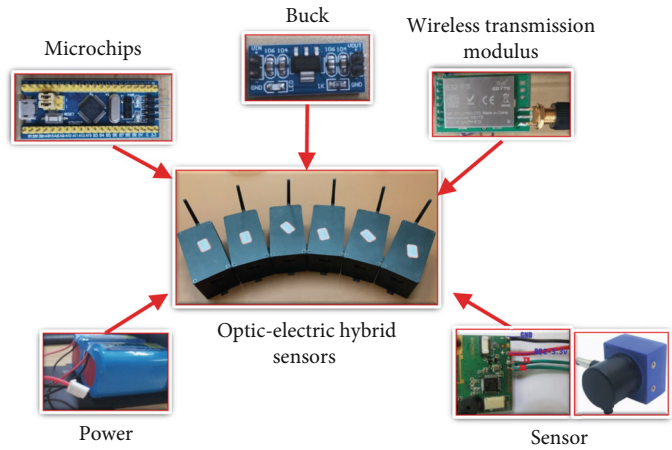

Figure 3: Hardware parts of the optic-electric hybrid sensing.

Figure 4: Intelligent control warning node.

conducted in a way that the reflector was set as a distance of 5 m, 30 m and 50 m, then it was moved in the range of 0 ~ 60 mm. The displacement was measured with a dial indicator. Then, the results of sensors were compared with the measurement of dial gauges which were shown in Figure 6. It can be seen from the figure that the actual displacement and the displacement measured by the infrared laser range finder have a good linear relationship. With the increasing of measurement distances, the linear relationship did not diverted which indicated the sensors were capable of measurement deformations at a long distance.

The calibration results of three cable convergence sensors are shown in Figure 6(a). It can be found that the actual displacement which was measured by the commercial linear variable differential transformer (LVDTs) and the displacement measured by the cable convergence instrument had a good linear relationship. The statistical histogram of the error frequency of each convergent was shown in the figure. The distribution of the measurement error was presented in Figure 6(b). From the 120 measurement results, the ranging error of each convergent was between -2 and 4 mm.

The probability density curve of measurement errors for optic-electric hybrid sensing nodes (i.e. No.1, 3, 5, 7, 9 and 11) are shown in Figure 7. Herein, the label of sensor node was defined for conveniences in the following field applications. The average errors of the laser rangefinders were -0.072 mm, 0.273 mm, -0.035 mm, 0.129 mm, 0.225 mm, and -0.260 mm with the corresponding standard deviations of 0.726, 0.767, 0.746, 0.793, 0.879, and 1.193 for hybrid sensing nodes No.1, 3, 5, 7, 9 and 11, respectively. It can be found from the results that the errors of No. 1, No. 3 and No. 5 ranged from -2 and 2 mm. However, the errors can be reduced by multiple measurements. Laboratory results shown that the average value of the measurement data can effectively reduce the measurement error. Therefore, after the infrared laser range finder and the cable convergence meter enter the ranging mode, the range was measured continuously 5 times. The distance data was transmitted to the intelligent control center. Then, the average measurement results were stored accordingly. Considering the external interference during the measurement, the measurement was repeated 5 times if the difference between the first data and the fifth data was greater than 3 mm.

3.2. Stability Analysis. The stability of data acquisition and transmission of the intelligent control monitoring system under long-term conditions was examined in this study. During the long-term condition test, the data acquisition was set up as 30 m away from the hybrid sensors. The data was recorded at each 15 minutes. Figure 8 shows variation of the measurement errors as compared with the LVDTs. Due to the limitation of laboratory tests, the measured results in a period of 600 minutes were used for the following analysis. Measurement over this time period can be represented for the performance analysis. The results indicated that the data drift of infrared laser rangefinders were ranged from -1 to 1 mm. The reason for the data drift may be attributed to the refraction of the laser in the air during the long-term work. It can be found that the measurement data of each infrared laser rangefinder was quite stable during long-term measurement.

4. Field Applications

The Intelligent monitoring and early-warning system was installed in the tunnel to monitor the uneven settlement of the Hongshan Road Station to Xiaohongshan Station in the t Metro Line 8, Wuhan, China. A new set of monitoring

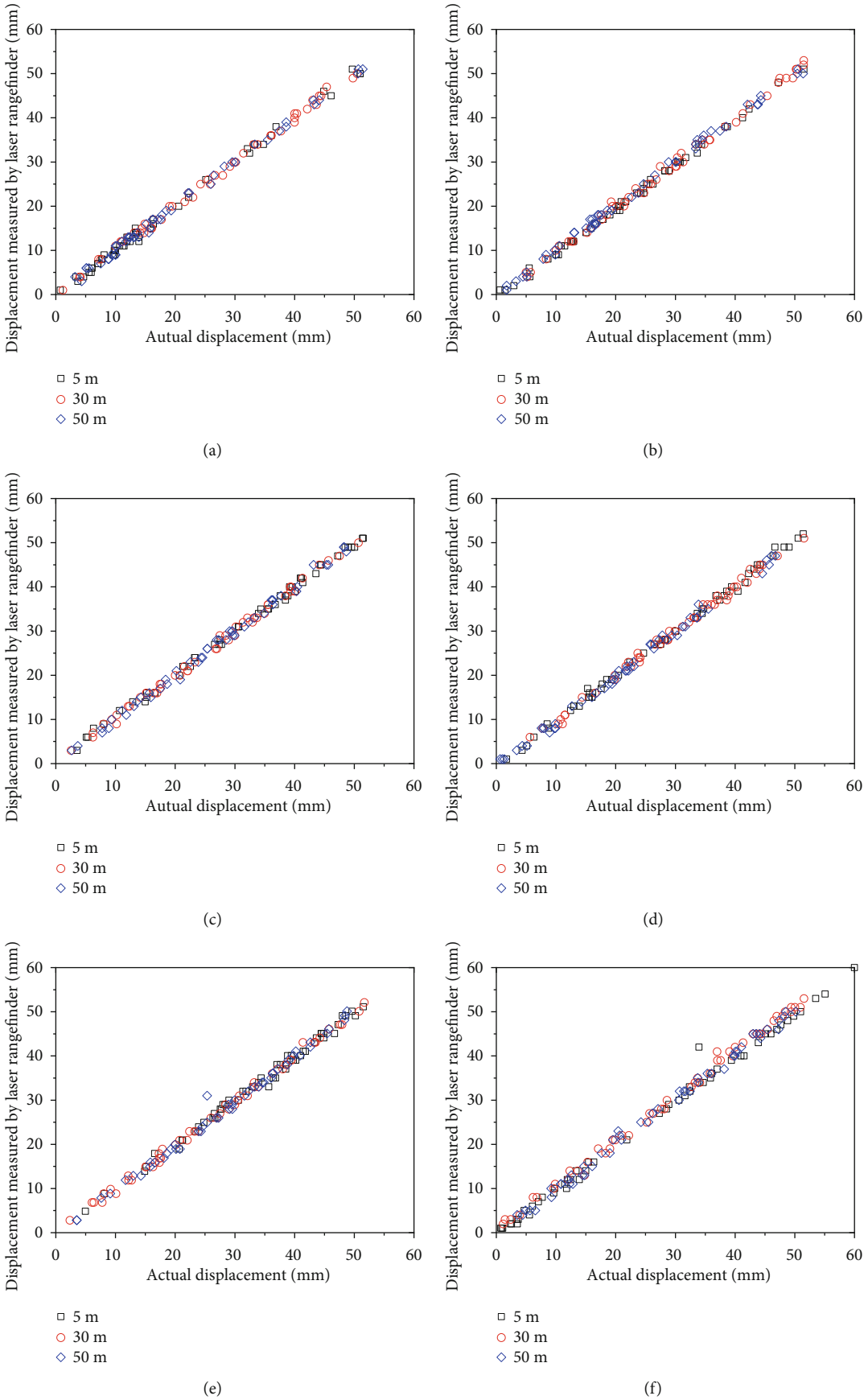

Figure 5: Calibration results of optic-electric hybrid sensors: (a) 1#; (b) 3#; (c) 5#; (d) 7#; (e) 9#; (f) 11#.

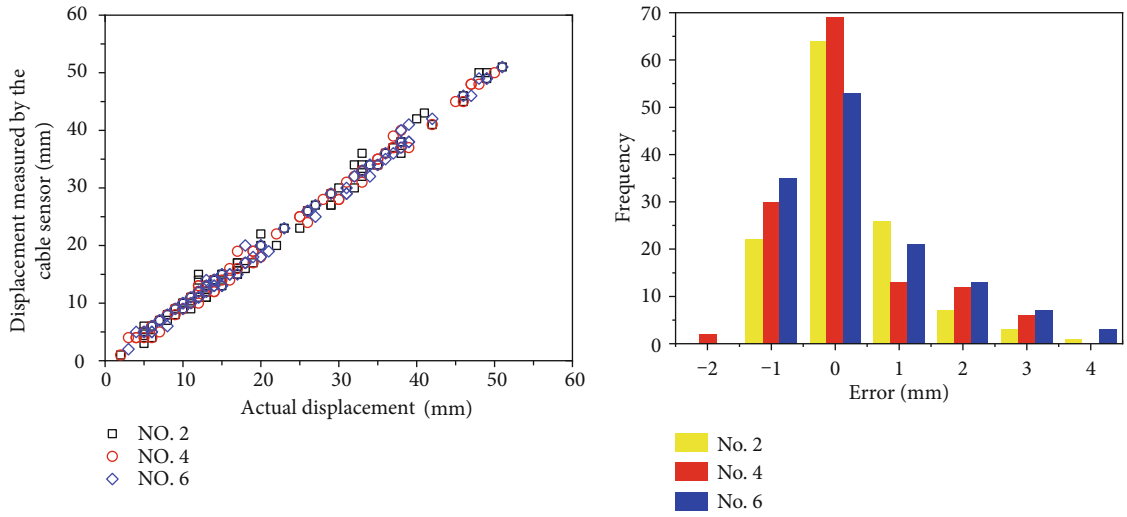

Figure 6: Statistic analysis of calibration results.

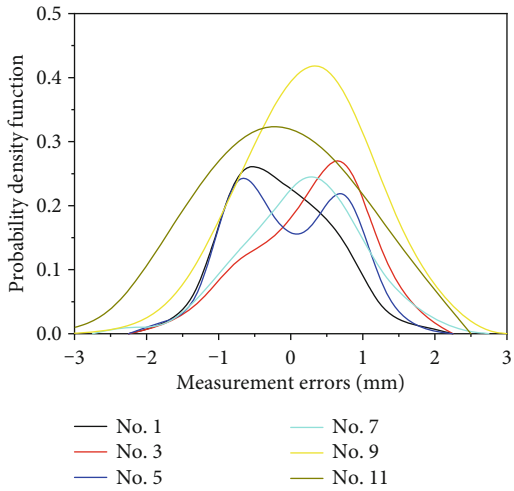

Figure 7: PDF of the measurement errors.

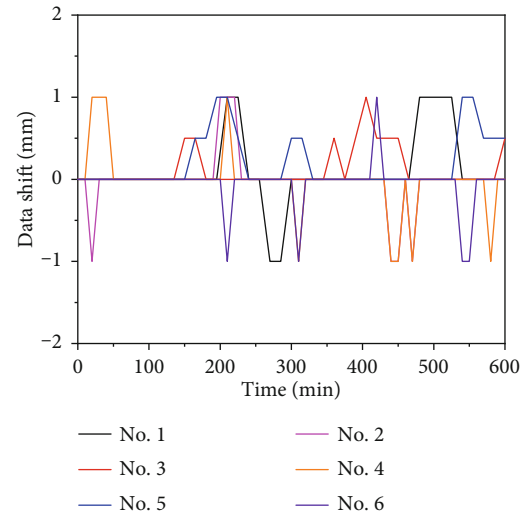

Figure 8: Stability analysis of hybrid sensors.

methods for the uneven settlement of the tunnel was proposed to study and analyze the settlement of the subway tunnel.

4.1. Project Background. The whole system was adopted in a under construction subway tunnel at the left line of Hongshan Road Station to Xiaohongshan Station in the third phase of the Metro Line 8, Wuhan, China, as shown in Figure 9. The instrumented section of the subway tunnel was constructed by the shield method. The large-section of the tunnel was 109 m in length, 20.14 m in width and 12.83 m in height, which has a cross section area of 258.40 square meters. It was currently the largest subway tunnel section in Wuhan. Due to the tunnel located in a karst area, the geological radar was used to detect the surrounding rock in advance. Apart from that, the shield deformation of the tunnel was critical for safety evaluation during construction. Thus, the hybrid sensors were installed in the tunnel for longitudinal and convergence deformation measurements. A remote real-time intelligent control center was installed around 50 m far from the measurement section. The frequency of data acquisition was determined by the control center. All the measurement results can be stored in the center and transmitted to the data servers for further analysis.

4.2. Field Instrumentations. The longitudinal and convergence deformations of subway tunnels were the key parameters for health evaluation. In this study, the longitudinal deformation along the tunnel was measured by the quasi-distributed optic-electric hybrid sensors, which were installed as shown in Figure 10. The sensor node 1 was installed at the gate of the subway tunnel as a reference point which was assumed no settlement during the whole monitoring period.

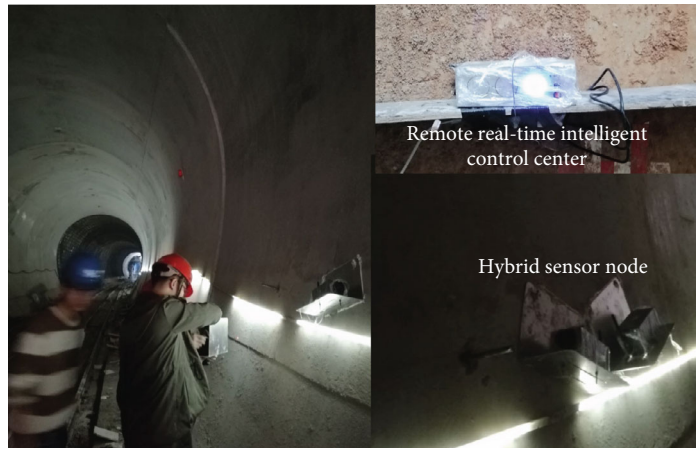

Figure 9: Photos of field instrumentations.

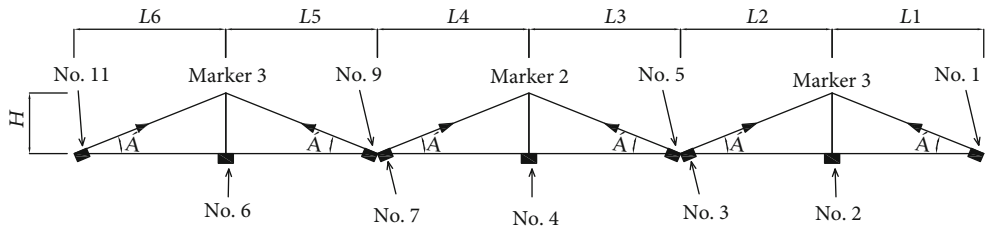

Figure 10: Diagram of sensor arrangements for field instrumentation.

The sensor node 3, 5, 7, 9 and 11 were distributed installed with inclined angle (i.e. α) of 22 degrees as presented in Figure 10. The reflectors installed on the upper side of the tunnel were used for the laser enhancement of the optic-electric hybrid sensors. Thus, the longitudinal deformation can be calculated by considering the relative deformation between sensor nodes. As shown in Figure 10, the horizontal and vertical distance between sensor nodes can be calculated by:

$$H = d * \sin \alpha \quad (1)$$

$$L = d * \cos \alpha \quad (2)$$

where d was the distance parameter measured by the infrared laser rangefinder, α was the initial elevation angle of the infrared laser rangefinder, and H and L were the horizontal and vertical distance between sensor nodes as shown in Figure 10, respectively. It should be noted that the optic-electric hybrid sensors were installed with a special designed L-shaped aluminum plate which cloud adjust the angle during the installation for various tunnel sections. A spatial coordinate system was established according to the installation parameters and the initial distance of each sensor nodes. Using the changes of coordinate in each measuring point, the settlement deformation curve of the tunnel can be determined. Therefore, the longitudinal deformation of the tunnel can be obtained thought the measured distances between the sensor nodes and the corresponding reflectors. All the monitoring data were transmitted to the edge computing and monitoring center.

4.3. Results Analysis. The optic-electric hybrid sensors and the intelligent control and monitoring system were installed in the under construction subway tunnel. Table 1 shows the following data collected in November 2019 and December 2019, respectively. The results of optic-electric hybrid sensors were recorded by the intelligent edge computing node. The real-time settlements and deformations of the tunnel were also calculated by the measured data with a spatial coordinate system.

Taking the optic-electric hybrid sensor No. 1 as a stable point, a spatial coordinate system was established by considering the longitudinal direction along the tunnel was the x-axis direction. The vertical ground upward was set as the y-axis positive direction. The coordinates of target No. 1 were determined by the coordinates of each point according to formula (1) and formula (2). The coordinates of target No. 3 were determined by the coordinates of infrared laser rangefinder No. 1. At the same time, the coordinates of each cable convergence instrument can be determined from the coordinates of the target.

Figure 11 shows the measured coordinate of each optic-electric hybrid sensor. As indicated in the figure, the coordinate values of Marker 1 were determined by the measured results of sensor No. 1 and No. 2. The following coordinate results can be derived with the same principles. The calculated coordinates of each measuring point were shown in Table 2. Since the tunnel was under construction, the overall deformation was critical for health evaluation. It should be noted that the measurement errors would be accumulated.

Table 1: Measured distances from the optic-electric hybrid sensors.

Sensor node	Incline angle/°	Results		Sensor node	Results	
		2019.11/m	2019.12/m		2019.11/m	2019.12/m
1#	22	5.237	5.235	2#	0.375	0.373
3#	22	5.465	5.466	4#	0.279	0.274
5#	22	5.116	5.110	6#	0.136	0.133
7#	22	5.895	5.897	9#	5.211	5.213

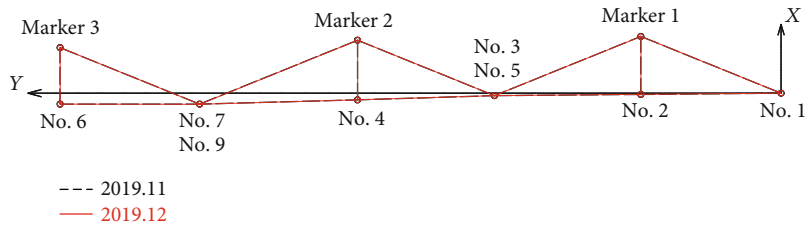

Figure 11: Measured results with spatial coordinate.

Table 2: Measured spatial coordinates.

Nos.	Initial 2019.11	Results 2019.12	Nos.	Initial 2019.11	Results 2019.12
1#	(0,0)	(0,0)	2#	(4.855,-0.043)	(4.853,-0.042)
3#	(9.921,-0.086)	(9.920, -0.087)	4#	(14.663,-0.232)	(14.657,-0.230)
5#	(9.921,-0.086)	(9.920, -0.087)	6#	(24.959,-0.378)	(24.956,-0.378)
7#	(20.128,-0.378)	(20.123,-0.382)	Mark 1	(4.855,1.964)	(4.853,1.963)
9#	(20.128,-0.378)	(20.123,-0.382)	Mark 2	(14.663,1.833)	(14.657,1.830)
—	—	—	Mark 3	(24.959,1.576)	(24.956,1.573)

Thus, it is significant to calibrate in a closed loop during measurement. If the difference was greater than 2% for the closed loop tests, the whole system would be self-verified and the errors would be eliminated accordingly in the algorithm.

5. Conclusions

The optic-electric hybrid sensor was proposed in this study for the settlement and deformation monitoring of subway tunnels. The hybrid sensor was combined the optic laser and electrical sensing technology with real-time monitoring and on-site edge computing. The working principle, system diagram, hybrid sensor prototype and field application were presented in this study. The remote wireless data transmission and early warning system were also employed in the whole system. Finally, the whole system was verified in a field construing subway tunnel at Xiaohongshan Station of Wuhan Metro Line No. 8, China. The major findings are listed as follows.

(1) The optic-electric hybrid sensor was developed with the merits of high accuracy, real-time monitoring, long distances (i.e. up to 50 m) and low cost. The hybrid sensor was calibrated in various conditions to prove the measurement accuracy. The sensor could be communicated with the edge computing node which has the intelligent algorithm to improve the stability and accuracy

(2) The intelligent algorithm can process and analyze abnormal data which would be deleted and additional measurement would be taken to substitute the abnormal result which was greatly improve the accuracy of the monitoring process and reduce the risk caused by the measurement errors. Calibration results shown that the accuracy of the hybrid sensor can reach 1 mm

(3) The intelligent control system realized the real-time measurement, wireless transmission, edge computing and sate of health evaluation. The measured results of hybrid sensors were transmitted to the control system for computing the settlement and deformations of subway tunnels

(4) The monitoring system was simple to operate, convenient to install, and relatively low in cost. It has good applicability in the construction and operation of the tunnel. The proposed system could provide useful guidance for tunnel excavation and deformation measurement during constructions and in service.

Data Availability

The [DATA TYPE] data used to support the findings of this study are available from the corresponding author upon request.

Conflicts of Interest

The authors declare no conflict of interest.

Authors' Contributions

Fu-guagn Zhu and Dong-sheng Xu designed the experiments, analyzed the data and wrote the paper. Ruishan Tan, Bin Peng, He Huang, and Zhuo-wen Liu are closely involved in lab tests and helped in writing the paper.

Acknowledgments

The financial supports of a research grant from National Natural Science Foundation of China (project No. 41972271) and the Fundamental Research Funds for the Central Universities, WHUT (Wuhan University of Technology, project No. 193106001) were gratefully acknowledged.

References

[1] H. Luo, Y. B. Chen, and H. E. Gang, "Benefit analysis of automatic deformation monitoring technology for mountain tunnels in Southwest China," *Tunnel Construction*, vol. 39, pp. 1277–1283, 2019.

[2] X. Y. Xie and Y. U. HJ, "Underneath tunnel deformation monitoring and control during deep excavation," *Chinese Journal of Underground Space and Engineering*, vol. 10, pp. 1646–1652, 2014.

[3] D. S. Xu and J. H. Yin, "Analysis of excavation induced stress distributions of GFRP anchors in a soil slope using distributed fiber optic sensors," *Engineering Geology*, vol. 213, pp. 55–63, 2016.

[4] D. S. Xu, "A new measurement approach for small deformations of soil specimens using fiber bragg grating sensors," *Sensors*, vol. 17, no. 5, p. 1016, 2017.

[5] D. S. Xu, L. J. Dong, L. Borana, and H. B. Liu, "Early-warning system with quasi-distributed fiber optic sensor networks and cloud computing for soil slopes," *IEEE Access*, vol. 5, pp. 25437–25444, 2017.

[6] D. S. Xu, F. B. Zhu, B. Lalit, X. C. Fan, and Q. B. Liu, "Construction solid waste landfills: risk assessment and monitoring by fibre optic sensing technique," *Geomatics, Natural Hazards and Risk*, vol. 12, no. 1, pp. 63–83, 2021.

[7] J. Y. Tang, D. S. Xu, and H. B. Liu, "Effect of gravel content on shear behavior of sand-gravel mixture," *Rock and Soil Mechanics*, vol. 39, no. 1, pp. 93–102, 2018.

[8] H. F. Pei, P. Cui, J. H. Yin et al., "Monitoring and warning of landslides anddebris flows using an optical fiber sensor technology," *Journal of Mountain Science*, vol. 8, pp. 728–738, 2011.

[9] D. A. Tibaduiza, R. Gomez, C. Pedraza, D. Agis, and F. Pozo, "Damage identification in structural health monitoring: a brief review from its implementation to the Use of data-driven applications," *Sensors*, vol. 20, no. 3, 2020.

[10] H. H. Zhu, B. Shi, J. Zhang, J. F. Yan, and C. C. Zhang, "Distributed fiber optic monitoring and stability analysis of a model slope under surcharge loading," *Journal of Mountain Science*, vol. 11, no. 4, pp. 979–989, 2014.

[11] D. Agis and F. Pozo, "A frequency-based approach for the detection and classification of structural changes using t-SNE," *Sensors*, vol. 19, no. 23, p. 5097, 2019.

[12] X. Y. Xie, X. Z. Lu, and H. Y. Tian, "Development of a modeling method for monitoring tunnel deformation based on terrestrial 3d laser scanning," *Chinese Journal of Rock Mechanics and Engineering*, vol. 32, pp. 2214–2224, 2013.

[13] S. T. Liu and G. R. Pan, "Sources of errors and deformation analysis of laser scanning based tunnel deformation monitoring," *Journal of Railway Engineering Society*, vol. 30, pp. 69–74, 2013.

[14] P. Dong, K. W. Xiao, and C. Y. Yu, "Monitoring and analysis of stratum deformation and subsidence overlying a shallow tunnel using distributed optical fiber sensing technology," *Journal of Disaster Prevention and Mitigation Engineering*, vol. 39, no. 5, pp. 724–732, 2019.

[15] G. Y. Hou, Z. X. Li, and T. Hu, "Research on tunnel settlement and deformation monitoring based on distributed optic fiber strain sensing technology," *Rock and Soil Mechanics*, vol. 9, 2020.

[16] Y. G. Du, M. Hu, and L. Teng, "Study of tidal fluctuation induced deformation law of a river-crossing shield tunnel in Shanghai," *Tunnel Construction*, vol. 37, no. 11, pp. 1424–1429, 2017.

[17] X. Yang, *Research on Non-uniform Settlement and Real-Time Monitoring Method of Shield Tunnel*, Beijing Jiaotong University, Ph. D thesis, Beijing, 2013.

[18] D. S. Xu, M. Huang, and Y. Zhou, "One-dimensional compression behavior of calcareous sand and marine clay mixtures," *International Journal of Geomechanics, ASCE*, vol. 20, no. 9, 2020.

[19] D. S. Xu, X. Y. Xu, W. Li, and B. Fatahi, "Field experiments on laterally loaded piles for an offshore wind farm," *Marine Structures*, vol. 69, p. 102684, 2020.

[20] S. Q. Zhang and H. F. Pei, "Rate of capillary rise in quartz nanochannels considering the dynamic contact angle by using molecular dynamics," *Powder Technology*, vol. 372, pp. 477–485, 2020.

[21] H. Pei, J. Jing, and S. Zhang, "Experimental study on a new FBG-based and Terfenol-D inclinometer for slope displacement monitoring," *Measurement*, vol. 151, p. 107172, 2020.

[22] H. Song, H. Pei, D. Xu, and C. Cui, "Performance study of energy piles in different climatic conditions by using multisensor technologies," *Measurement*, vol. 162, p. 107875, 2020.

[23] D. S. Xu, J. Y. Tang, Y. Zhou, R. Rui, and H. B. Liu, "Macro and micro investigation of gravel content on simple shear behavior of sand-gravel mixture," *Construction and Building Materials*, vol. 221, pp. 730–744, 2019.

[24] D. S. Xu, H. B. Liu, R. Rui, and Y. Gao, "Cyclic and postcyclic simple shear behavior of binary sand-gravel mixtures with various gravel contents," *Soil Dynamics and Earthquake Engineering*, vol. 123, pp. 230–241, 2019.

[25] D. S. Xu, Z. Y. Tang, and L. Zhang, "Interpretation of coarse effect in simple shear behavior of binary sand-gravel mixture by DEM with authentic particle shape," *Construction and Building Materials*, vol. 195, pp. 292–304, 2019.

[26] D. S. Xu, H. B. Liu, and W. L. Luo, "Evaluation of interface shear behavior of GFRP soil nails with a strain-transfer model and distributed fiber-optic sensors Computers and Geotechnics," *Computers and Geotechnics*, vol. 95, pp. 180–190, 2018.

[27] D. S. Xu, H. B. Liu, and W. L. Luo, "Development of a novel settlement monitoring system using Fiber-optic liquid-level transducers with automatic temperature compensation," *IEEE Transactions on Instrumentation and Measurement*, vol. 67, no. 9, pp. 2214–2222, 2018.

[28] D. S. Xu, "A new measurement approach for deflection monitoring of large-scale bored piles using distributed fiber sensing technology," *Measurement*, vol. 117, no. 3, pp. 444–454, 2018.

[29] K. Meng, C. Y. Cui, and H. J. Li, "An ontology framework for pile integrity evaluation based on analytical methodology," *IEEE Access*, vol. 8, pp. 72158–72168, 2020.

[30] Y. Vidal, G. Aquino, F. Pozo, and J. E. M. Gutiérrez-Arias, "Structural health monitoring for jacket-Type offshore wind turbines: experimental proof of concept," *Sensors*, vol. 2020, 1835.